


RESEARCH

Open Access



Development a glycosylated extracellular vesicle-derived miRNA Signature for early detection of esophageal squamous cell carcinoma

Jianlin Chen^{1,2†}, Yue Zheng^{1,2†}, Zhen Wang^{3†}, Qi Gao⁴, Kun Hao⁵, Xiongfeng Chen^{1,6}, Nantian Ke^{1,2}, Xiang Lv^{1,2}, Jiamiao Weng^{1,2}, Yuhong Zhong⁷, Zhixin Huang^{2,8}, Miao Fu⁹, Lilan Zhao^{1,10}, Fan Lin^{1,11,12}, Hui Mi¹³, Haijun Tang^{1,14*}, Chundong Yu^{1,14,15*} and Yi Huang^{1,2,14,16,17*} 

Abstract

Background Esophageal squamous cell carcinoma (ESCC) is often diagnosed at an advanced stage due to the lack of non-invasive early detection tools, which significantly impacts patient prognosis. Given that glycosylation alterations especially high sialylation and fucosylation, frequently occur during cellular malignant transformation, but their roles are not elucidated. We examined alterations in disease-specific glycosylated extracellular vesicles (EVs)-derived miRNAs in the serum of ESCC patients, evaluating their utility as diagnostic biomarkers.

Methods A total of 371 ESCC and 303 healthy controls (HCs) were recruited in this multi-stage, multicentre case-control study. Fucosylated (Fuc-) and sialylated (Sia-) EVs were isolated utilizing Lentil lectin (LCA) and wheat germ lectin (WGA)-coated magnetic beads, respectively. The glycosylated EVs-derived miRNAs-based signature (Riskscore^{Fuc-&Sia-}) was established through logistic regression in a training cohort and subsequently validated in an internal and an external multicentre cohort.

Results The Riskscore^{Fuc-&Sia-} effectively identified ESCC across all stages, demonstrating high AUC values in training (0.980), internal validation (0.957), and external multicentre validation (0.973) cohorts, markedly higher than carcinoembryonic antigen (CEA) (AUC = 0.769, training cohort; AUC = 0.749, internal validation cohort; AUC = 0.765, external validation cohort). Notably, this score exhibited robust accuracy in detecting CEA (-) ESCC cases (CEA < 5 ng/ml) (AUC = 0.974, training & internal cohort; AUC = 0.973, external multicentre validation cohort). Additionally, it displayed strong efficacy in differentiating early-stage ESCC patients (AUC = 0.982, training cohort; AUC = 0.977, external multicentre validation cohort).

[†]Jianlin Chen, Yue Zheng and Zhen Wang contributed equally to this work.

*Correspondence:

Haijun Tang
tanghaijun16@163.com
Chundong Yu
cdyu@xmu.edu.cn
Yi Huang
hyi8070@126.com

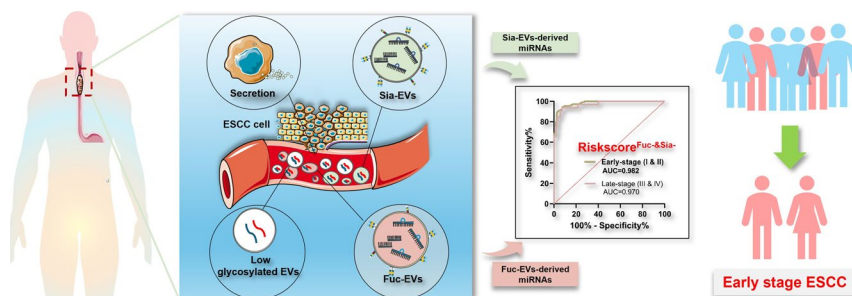
Full list of author information is available at the end of the article



Conclusions Our study illustrates the effectiveness of glycosylated EVs capture strategy for isolating tumour-specific EVs. The unique glycosylated EVs-derived miRNAs-based signature shows the optimal potential as a biomarker for early detection of ESCC.

Keywords Glycosylated EVs capture, miRNA, Liquid biopsy, Early diagnosis, Esophageal squamous cell carcinoma

Graphical Abstract



Background

Esophageal squamous cell carcinoma (ESCC) is predominantly found in non-western nations, with more than half of the global cases concentrated in China [1]. In 2020, China reported 324,422 new cases of ESCC, positioning it as the sixth most frequently diagnosed cancer in the country [2]. Although advancements in treatment have been made, the five-year survival rate remains low, at 15% to 25%, due to late-stage diagnosis [3]. The consolation is that ESCC patients at early stage, who receive prompt treatment have a higher 5-year survival rate [4, 5]. Thus, early detection and timely intervention are crucial for enhancing the survival outcomes of individuals with ESCC.

At present, endoscopy and mucosal biopsy are considered to be effective diagnostic methods for ESCC, but they cannot be used for routine screening of ESCC patients due to disadvantages such as high cost, relatively complex operation and uncomfortable invasion experience [6]. In recent years, serological biomarkers, such as carcinoembryonic antigen (CEA), squamous cell carcinoma antigen (SCC-Ag) continue to be the most extensively researched and widely utilized markers in patients with ESCC [7–10]. However, both exhibit varying levels of sensitivity and specificity for identification and early differentiation of ESCC [7–10]. Therefore, novel diagnostic strategies for the early detection of primary ESCC are urgently needed.

In recent years, the detection of circulating tumour cells (CTCs), circulating tumour DNA (ctDNA), and extracellular vesicles (EVs) in liquid biopsy has garnered increasing attention, with potential applications in early cancer

detection and disease monitoring [11, 12]. Nonetheless, CTCs present challenges due to their scarcity, heterogeneity, and the complexities involved in their isolation and characterization [13]. Similarly, ctDNA is characterized by high fragmentation, low abundance, and instability, which constrain its utility [14, 15]. Conversely, EVs secreted by cancer cells possess cancer-specific components that can be readily isolated from bodily fluids. Furthermore, EVs offer significant advantages due to their abundant presence in plasma and other bodily fluids (10^8 - 10^{13} /ml), as well as their stability, ease of acquisition, and correlation with tumour characteristics [16, 17]. In recent years, EVs have garnered increasing attention as a promising biomarker source for the liquid biopsy of cancer. Therefore, how to effectively capture and enrich tumour-derived EVs followed by further identification of candidate EVs cargoes for tumours from the complex blood system is of great significance for improving the early diagnosis efficiency of patients with malignant tumours. Traditional separation methods are mainly based on the physical properties of EVs and cannot distinguish well between tumour-derived EVs and benign EVs [18, 19]. It's interesting that in recent years abnormal glycosylations have been shown to be closely related to the occurrence, malignant differentiation, metastasis, and development of tumours [20–22]. Of particular note are sialylation and fucosylation, two prevalent glycosylation modifications that have been extensively studied for their heightened expression in tumour cells and tumour-derived EVs, rendering their significant role in biomarkers for cancer development [23–25]. Our research team recently developed a diagnostic model for early detection of lung adenocarcinoma by isolating fucosylated

EVs [26]. Further investigation has revealed that increased levels of tumour-suppressing miR-4732-3p in serum fucosylated EVs indicate a phenomenon termed "exosome escape," which may serve as a potential diagnostic indicator for non-small cell lung cancer (NSCLC) and for monitoring the advancement of the disease [25]. It suggests that glycosylated EVs play a crucial role in the development and metastasis of cancer, so it holds promise for liquid biopsy-based glycosylated EVs biomarker discovery for cancer diagnosis. Considering the increasing prevalence of ESCC and the challenges in its early diagnosis, this research conducted a comprehensive exploration to thoroughly ascertain the glycosylated EVs-derived miRNAs-based signature (RiskScore^{Fuc-&Sia-}) for the early diagnosis of ESCC. After the identification of biomarkers, we meticulously validated these signatures in various independent patient cohorts and successfully developed an innovative liquid biopsy test for the early identification of individuals with initial-stage ESCC.

Methods

See the detailed in Methods in the Additional file1.

Results

Identification and selection of candidate miRNAs and potential differentially expressed miRNAs (pDEmiRNAs)

We successfully isolated EVs using glycosylation capture strategies. The automated workflow takes advantage of tumour-derived EVs isolation, which greatly improves the speed, efficiency, and throughput (Additional file 1: Fig. S1). Comprehensive clinical data of the individuals involved in this study are summarized in Table 1. To further explore the diagnostic value of glycosylated EVs-derived miRNAs in ESCC, we designed a five-step process, including biomarker discovery, screening, training, internal validation, and external validation (Fig. 1A). Detailed marker screening criteria and processes are shown in Additional file 1: Fig. S2. The sequencing data were normalized and summarized in Additional file 2: Table S1-2.

In the analysis of small RNA sequencing, a total of 1060 Fuc-EVs miRNAs were detected. Of these, 27 miRNAs displayed varying levels of expression between the ESCC and HC groups, with 14 miRNAs showing upregulation ($p < 0.05$, and $\log_2 \text{FC} > 1.5$; Additional file 2: Table S3). A volcano plot illustrating these miRNAs is presented in Fig. 1B. Additionally, hierarchical clustering of the 16 participants based on the expression levels of 10 Fuc-EVs-derived candidate miRNAs revealed two separate groups, as depicted in Fig. 1C. A total of 494 Sia-EVs miRNAs were identified, with 6 candidate miRNAs specifically obtained

($p < 0.05$, and $\log_2 \text{FC} > 1.5$; Additional file 2: Table S3). The volcano plots and clustering plots illustrating these miRNAs are depicted in Fig. 1D-E. Following the outlined criteria, 16 candidate miRNAs were identified, including 10 Fuc-EVs-derived miRNAs and 6 Sia-EVs-derived miRNAs (Table 2).

Among the ten Fuc-EVs-derived candidate miRNAs, the quantities of miR-1228-5p, miR-6842-3p, miR-582-3p, miR-548o-3p, miR-642a-3p, and miR-30e-3p still exhibited an upwards trend, while the expression levels of other candidate miRNAs remained unchanged (Additional file 1: Fig. S3A). RT-qPCR analysis also revealed significantly elevated levels of 6 Sia-EVs-derived candidate miRNAs (miR-2110, miR-425-5p, miR-939-5p, miR-652-3p, miR-874-3p, and miR-338-5p) in ESCC patients ($n = 24$) compared with healthy individuals in a screening cohort ($p = 0.024$, $p = 0.0002$, $p = 0.0431$, $p = 0.0318$, $p < 0.0001$, and $p < 0.0001$, respectively) (Additional file 1: Fig. S3B). Subsequently, a preliminary evaluation was carried out to determine the diagnostic potential of the candidate miRNAs within the screening cohort. A detailed overview of their diagnostic effectiveness is outlined in Additional file 1: Table S4. Based on established criteria, four Fuc-EVs-derived miRNAs (miR-1228-5p, miR-6842-3p, miR-30e-3p, and miR-642a-3p) and three Sia-EVs-derived miRNAs (miR-425-5p, miR-874-3p, and miR-338-5p) were categorized as pDEmiRNAs.

Evaluation of differentially expressed miRNAs (DEmiRNAs) in the training cohort and construction of diagnostic models

Consistent with the findings of the screening set, the pDEmiRNAs in the training sets exhibited consistent and significantly differential expression between ESCC patients and HCs (all $p < 0.001$, Additional file 1: Fig. S4A, C). Hence, we identified these seven pDEmiRNAs as DEmiRNAs, including four Fuc-EVs-derived miRNAs (miR-1228-5p, miR-6842-3p, miR-30e-3p, and miR-642a-3p) and three Sia-EVs-derived miRNAs (miR-425-5p, miR-338-5p and miR-874-3p). We also analysed the expression levels of CEA and SCC-Ag and revealed that both were elevated in ESCC patients compared to HCs (Additional file 1: Fig. S4B). The seven DEmiRNAs demonstrated significant discriminatory power between the ESCC patients and HCs, as evidenced by the ROC curves (Additional file 1: Fig. S4D-E). The corresponding AUCs were 0.869 for miR-642a-3p, 0.916 for miR-6842-3p, 0.792 for miR-1228-5p, 0.684 for miR-30e-3p, 0.762 for miR-425-5p, 0.829 for miR-338-5p, and 0.798 for miR-874-3p, suggesting their potential for further evaluation through the development of logistic regression models (Additional file 1: Table S5).

Table 1 Characteristics of all participants in the study

Variable	Discovery cohort		Screening cohort		Training cohort		Internal validation cohort		External validation cohort			
	Fuc-EVs: ESCC (n = 10)	Fuc-EVs: HC (n = 6)	Sia-EVs: ESCC (n = 12)	Sia-EVs: HC (n = 36)	ESCC (n = 24)	HC (n = 24)	ESCC (n = 160)	HC (n = 120)	ESCC (n = 60)	HC (n = 45)	ESCC (n = 105)	HC (n = 72)
Age, median (range)	63 (54–75)	55 (41–66)	65 (50–81)	47 (49–69)	66 (52–84)	60 (50–65)	67 (55–86)	58 (48–67)	64 (51–85)	55 (52–63)	68 (53–82)	61 (54–66)
Gender, n (%)												
Male	6(60)	4(66.66)	8(66.67)	25(69.44)	17(70.8)	15(62.5)	131(81.88)	95(79.17)	48(80)	37(82.22)	85(80.95)	58(79.46)
Female	4(40)	2(33.34)	4(33.33)	11(30.56)	7(29.2)	9(37.5)	29(18.12)	25(20.83)	12(20)	8(17.78)	20(19.05)	14(19.44)
Stage (TNM), n (%)												
I	4(40)		5(41.67)		11(45.83)		52(32.5)		19(31.67)		36(34.29)	
II	6(60)		7(58.33)		8(33.33)		59(36.86)		21(35)		44(41.90)	
III					3(12.5)		28(17.5)		13(21.67)		17(16.19)	
IV					2(8.33)		14(8.75)		7(11.67)		8(7.62)	
Unstaged							7(4.38)					

TNM tumor-node-metastasis, TNM stage was based on AJCC 7th edition

Fig. 1

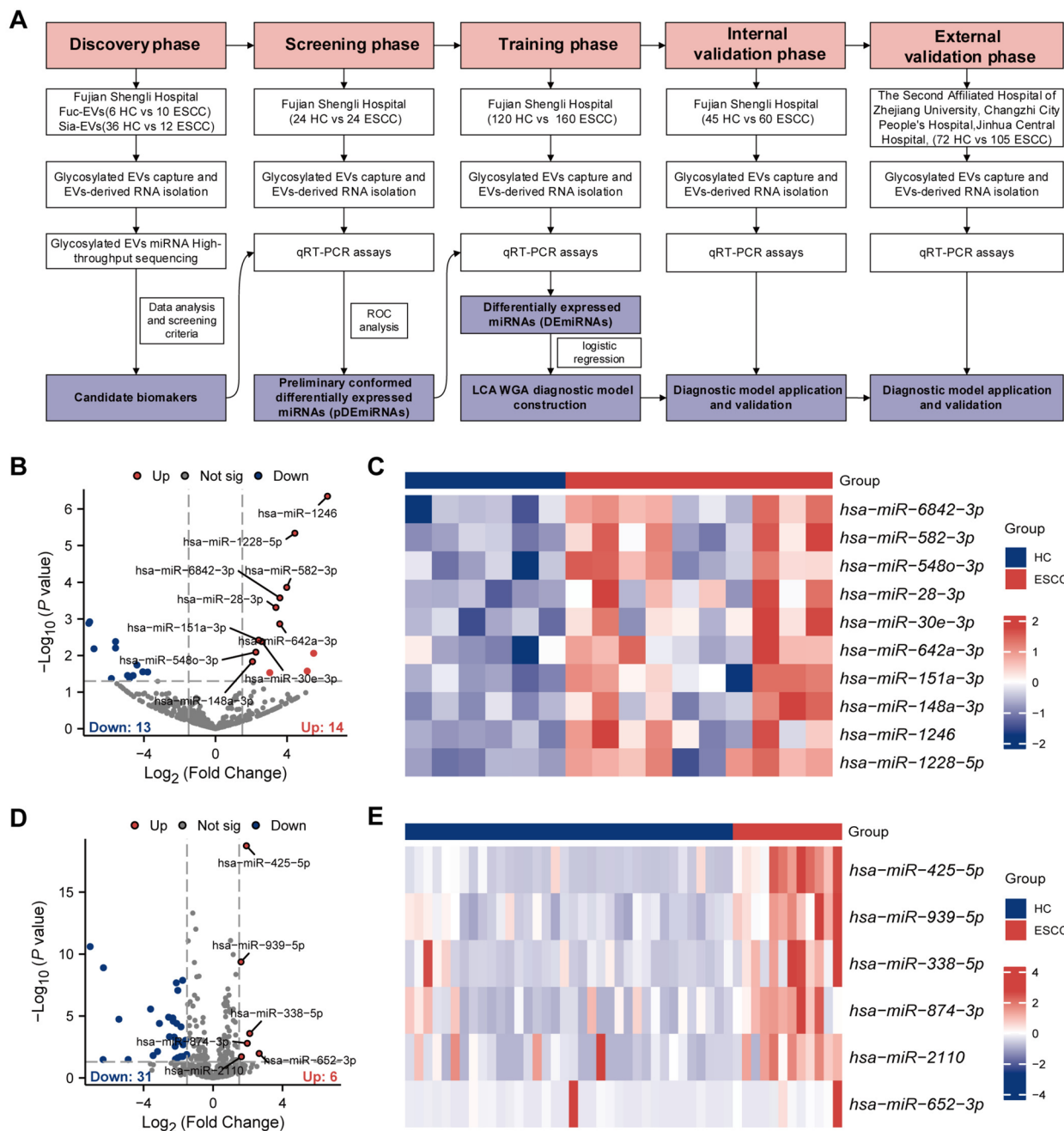


Fig. 1 The utilization of small RNA sequencing to identify glycosylated EVs-derived miRNAs for predicting patients with ESCC. **A** Flow diagrams showing the design of this study. **B** Volcano plot illustrates the significantly up and down regulated miRNAs derived from the Fuc-EVs discovery cohort ($n = 16$) based on the criteria ($|\log_2 \text{ fold change}| > 1.5$, and $p < 0.05$). **C** Heatmap representing of 10 Fuc-EVs-derived candidate miRNAs in serum samples from Fuc-EVs discovery cohort (ESCC = 10, HC = 6). **D** Volcano plot displaying miRNAs significantly up and down regulated in ESCC vs HC from the Sia-EVs discovery cohort ($n = 48$). **E** Heatmap depicts the 6 markedly upregulated Sia-EVs-derived miRNAs among the patients with ESCC and HCs in the Sia-EVs discovery cohort (ESCC = 12, HC = 36)

Based on the aforementioned validation results, three robust diagnostic models were further developed utilizing logistic regression analysis. Remarkably, the

glycosylated EVs-derived miRNA-based panels in the serum training cohort demonstrated exceptional diagnostic precision in patients with ESCC, with an AUC

Table 2 The candidate miRNAs from Fuc-EVs and Sia-EVs

miRNA	base Mean	log2FoldChange	p value
Fuc-EVs-derived candidate miRNAs			
hsa-miR-1246	356.33	6.26	<0.001
hsa-miR-1228-5p	510.74	4.43	<0.001
hsa-miR-582-3p	4006.84	3.98	<0.001
hsa-miR-6842-3p	467.08	3.60	<0.001
hsa-miR-642a-3p	4200.31	3.59	<0.001
hsa-miR-28-3p	1815.53	3.38	<0.001
hsa-miR-30e-3p	709.87	2.58	<0.001
hsa-miR-151a-3p	656.36	2.41	<0.001
hsa-miR-548o-3p	391.14	2.25	<0.001
hsa-miR-148a-3p	19,341.39	2.07	0.014
Sia-EVs-derived candidate miRNAs			
hsa-miR-652-3p	37.97	2.65	0.01
hsa-miR-338-5p	49.58	2.11	<0.001
hsa-miR-874-3p	30.01	1.96	<0.001
hsa-miR-425-5p	22,829.72	1.92	<0.001
hsa-miR-2110	31.11	1.63	0.01
hsa-miR-939-5p	282.49	1.61	<0.001

Fuc^- of 0.940 (95% CI: 0.91–0.97), an AUC Sia^- of 0.877 (95% CI: 0.83–0.91), and an AUC $Fuc^- \& Sia^-$ of 0.980 (95% CI: 0.96–0.99) (Fig. 2A–F, Table 3). The diagnostic outcomes and efficiency demonstrated in the training cohort warrant further validation through independent group evaluations.

Glycosylated EVs-derived miRNA-based panels robustly identified ESCC in an independent internal validation cohort and an external validation cohort from medical centres.

Subsequently, we verify the diagnostic performance of the built glycosylated EVs-derived miRNA-based panels in independent internal and external validation cohorts. In the internal validation cohort (HC=45, ESCC=60), the levels of biomarkers mirrored their expression trends observed in the training cohort, as depicted in Additional file 1: Fig. S5A–C. The findings revealed that the expression profiles of the seven glycosylated EVs DEmiRNAs as well as CEA linked to the external validation cohort ($n=177$, with 105 ESCC patients and 72 healthy controls) were in full alignment with their expression patterns observed during the training phase and internal validation phase (Additional file 1: Fig. S6A–C). The relative expression heatmaps of Fuc-EVs- and Sia-EVs-derived DEmiRNAs in independent internal and external validation cohorts are shown in Fig. 3A–B, both of which can well distinguish ESCC patients from healthy controls. ROC analysis was then conducted to assess the efficacy of individual Fuc-EVs-derived DEmiRNAs, SCC, and

Sia-EVs-derived DEmiRNAs in the diagnosis of ESCC in these two validation cohorts (Additional file 1: Fig. S5D–E, Table S6–7).

Moreover, upon establishing the risk prediction equations in the training set, their diagnostic efficacy was subsequently validated within this internal validation cohort. In line with the findings from the training set, the panels of biomarkers continued to demonstrate exceptional performance in distinguishing individuals with ESCC from healthy controls, with an AUC Fuc^- = 0.910, an AUC Sia^- = 0.875, and an AUC $Fuc^- \& Sia^-$ = 0.957 in an internal validation cohort (Fig. 3C, Table 3). No doubt about it, our distinctive signatures still effectively identified ESCC from healthy subjects, with an AUC Fuc^- = 0.925, an AUC Sia^- = 0.874, and an AUC $Fuc^- \& Sia^-$ = 0.973 in an external validation cohort. (Fig. 3D, Table 3).

Glycosylated EVs-derived miRNAs-based signature (RiskScore $Fuc^- \& Sia^-$) combines CEA in serum significantly improve diagnostic accuracy for ESCC

In routine clinical settings, SCC-Ag and CEA are commonly utilized as blood biomarkers for the management of patients with ESCC. Nevertheless, their limited sensitivity and specificity hinder their ability to effectively detect patients within a diverse population [27]. Consequently, the investigation of integrating glycosylated EVs-derived miRNAs-based signature with these traditional markers was undertaken to improve diagnostic precision in clinical contexts. Accordingly, serum levels of SCC-Ag and CEA were assessed in various cohorts, and their diagnostic efficacy for ESCC was also evaluated. Our data show that SCC-Ag has very poor diagnostic capabilities for ESCC [training cohort: AUC = 0.539(0.471–0.607); internal validation cohort: AUC = 0.561(0.451–0.671)] (Additional file 1: Table S5–6). Interestingly, CEA showed relatively stable AUC value at all stages of diagnosis in ESCC patients, showing moderate diagnostic ability [training cohort: AUC = 0.769 (0.715–0.824); internal validation cohort: AUC = 0.749 (0.656–0.844); external validation cohort: AUC = 0.765 (0.693–0.837)] (Fig. 4A–C, Additional file 1: Table S8). Therefore, we abandoned SCC-Ag and selected CEA for subsequent combined diagnostic studies. The results showed that in the training cohort, while CEA alone had an AUC of 0.769, combining it with our RiskScore $Fuc^- \& Sia^-$ led to a considerable enhancement in the aggregate diagnostic efficacy, achieving an AUC score of 0.989, was observed across all stages of patients with ESCC, and the advantages of this combination were also validated in internal validation cohort (AUC = 0.962) and external validation cohort (AUC = 0.983) (Fig. 4A–C, Additional file 1: Table S8). These findings suggest

Fig. 2

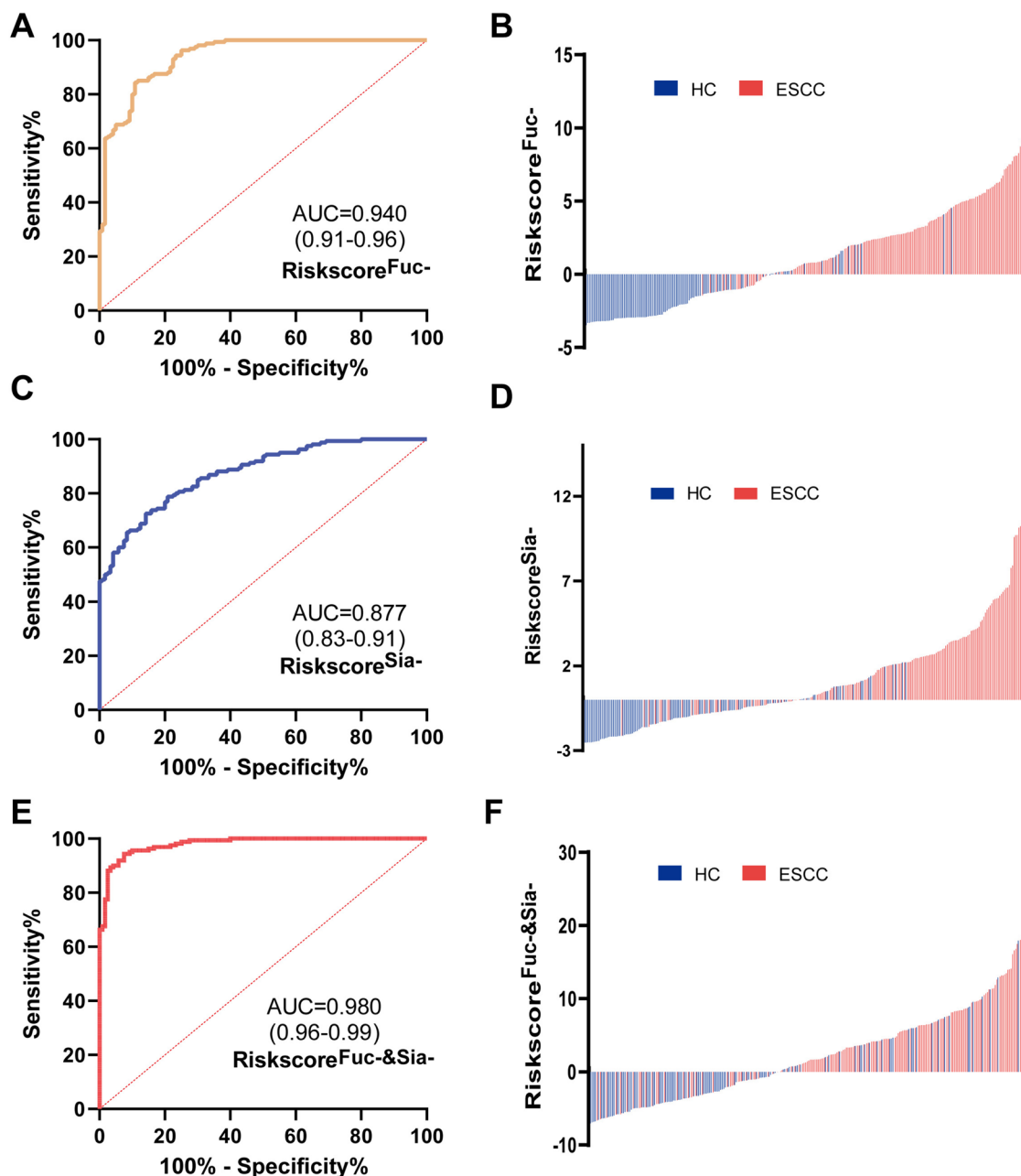


Fig. 2 Construction of glycosylated EVs DE miRNAs-based signatures and assessment of their diagnostic abilities in training cohort. ROC curve analysis (95% CIs) reveals the performance of the $Riskscore^{Fuc-}$ (A), $Riskscore^{Sia-}$ (C), and $Riskscore^{Fuc-\&Sia-}$ (E) in 160 ESCC and 120 HCs serum samples. The waterfall plot illustrates the $Riskscore^{Fuc-}$ (B), $Riskscore^{Sia-}$ (D), and $Riskscore^{Fuc-\&Sia-}$ (F) distribution between serum samples of patients with ESCC and HCs in the training cohort

that while our $Riskscore^{Fuc-\&Sia-}$ demonstrates strong reliability by itself, its integration with CEA levels markedly enhances diagnostic precision overall. This underscores its applicability in the clinical screening of individuals with ESCC.

In the existing clinical framework, diagnosing patients with ESCC relies on techniques such as imaging, invasive biopsy procedures, and, where applicable, surgical excision. Consequently, inaccuracies leading to false positives or negatives during the screening process can

Table 3 Summary of diagnostic performance of miRNA-based biomarker panel in the training and validation cohorts

Variable	Training cohort, % (CI)			Internal Validation cohort, % (CI)			External Validation cohort, % (CI)		
	Fuc-EVs-derived-DEmiRNAs panel	Sia-EVs-derived-DEmiRNAs panel	Fuc-&Sia-EVs-derived-DEmiRNAs panel	Fuc-EVs-derived-DEmiRNAs panel	Sia-EVs-derived-DEmiRNAs panel	Fuc-&Sia-EVs-derived-DEmiRNAs panel	Fuc-EVs-derived-DEmiRNAs panel	Sia-EVs-derived-DEmiRNAs panel	Fuc-&Sia-EVs-derived-DEmiRNAs panel
AUC	0.940 (0.914-0.966)	0.877(0.839-0.915)	0.980(0.968-0.993)	0.910(0.854-0.963)	0.875(0.811-0.939)	0.957(0.924-0.991)	0.925(0.888-0.963)	0.874(0.825-0.923)	0.974(0.954-0.993)
SE%	84.38	72.5	94.38	85	75	88.33	84.76	75.24	93.33
SP%	89.17	85.83	92.5	82.22	86.67	93.33	87.5	90.28	91.67
AC%	86.43	78.21	93.57	83.81	80	90.48	85.88	81.36	92.66
PPV%	91.22	87.22	94.38	86.44	88.24	94.64	90.82	91.86	94.23
NPV%	81.06	70.07	92.5	80.44	72.22	85.71	79.75	71.43	90.41
Youden Index%	73.54	58.33	86.88	67.22	61.67	81.67	72.26	65.52	85.00

AUC area under the curve, CI confidence interval, SE sensitivity, SP specificity, AC accuracy, NPV negative predictive value, PPV positive predictive value

Fig. 3

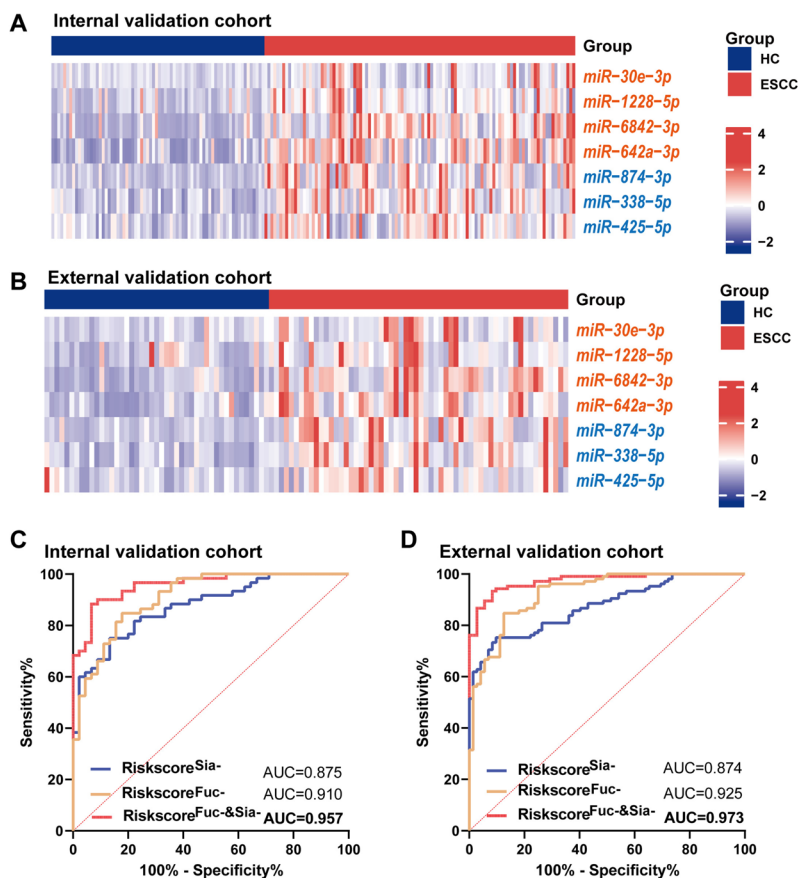


Fig. 3 Performance evaluation of glycosylated EVs DEmiRNAs-based panels in an internal validation cohort and in an external validation cohort by RT-qPCR. **A-B** Representative heatmap of 7 DEmiRNAs in patients with ESCC versus non-disease controls in internal validation cohort (**A**), and in external validation cohort (**B**). **C-D** ROC curves analysis for the Riskscore^{Fuc-}, Riskscore^{Sia-}, and Riskscore^{Fuc-&Sia-} in internal validation cohort (**C**), and in external validation cohort (**D**)

Fig. 4

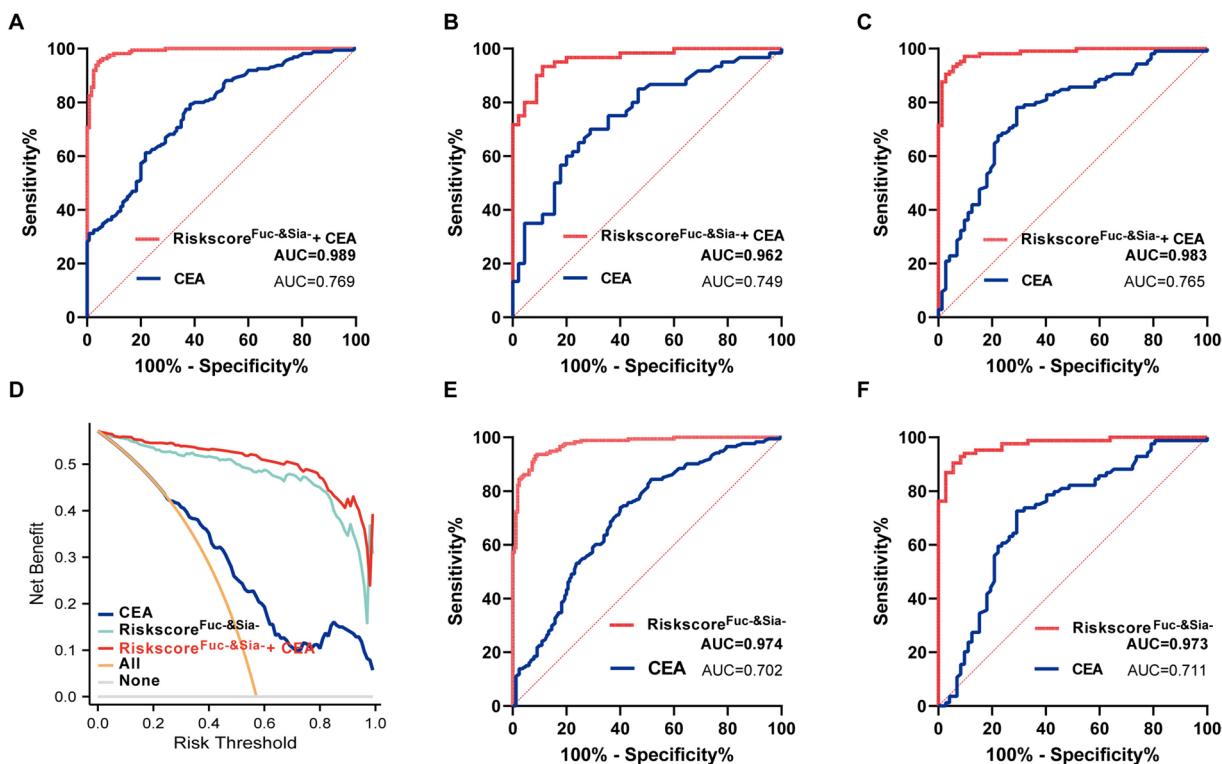


Fig. 4 Performance evaluation of the glycosylated EVs-derived miRNAs-based signature (RiskScore^{Fuc-&Sia-}) in combination with CEA, and diagnostic potential evaluation by decision curve analysis. **A-C** ROC analysis compared the diagnostic performance of CEA combined with RiskScore^{Fuc-&Sia-} and CEA alone for all stages of ESCC patients in training cohort (**A**), in internal validation cohort (**B**), and in external validation cohort (**C**). **D** Decision curve shows the net benefit curves for the RiskScore^{Fuc-&Sia-} alone, CEA alone, and the combined CEA and the RiskScore^{Fuc-&Sia-} in all stage ESCC patients from the training cohort. **E-F** Performance of RiskScore^{Fuc-&Sia-} in 338 participants (173 ESCC and 165 healthy controls) from training and internal validation cohorts who presented with all CEA level less than 5 ng/ml (**E**) and validated in 156 participants (84 ESCC and 72 healthy controls) from external validation cohort (**F**)

detrimentally affect individuals subjected to these assessments. Thus, the clinical value of different screening methodologies must be carefully weighed, balancing the potential harm against the diagnostic benefits. To assess the clinical relevance of our diagnostic model further, we conducted a decision curve analysis (DCA). The outcomes from the DCA indicate that the RiskScore^{Fuc-&Sia-} combined with CEA offered a superior net benefit vs the RiskScore^{Fuc-&Sia-} alone in the training cohort across most ranges of threshold probability for diagnosis all stage of ESCC, suggesting a more favourable balance between risk and diagnostic yield (Fig. 4D).

In clinical practice, we often encounter ESCC patients with CEA < 5 ng/ml, and this proportion accounts for almost 80% of the total ESCC patients, and our data should also prove this. Notably, in our training & internal validation cohorts, there were 173 out of 220 ESCC with a CEA level < 5 ng/ml. In our external

validation cohort, this proportion reached a staggering 80% (84/105). Herein, we interrogated the ability of our RiskScore^{Fuc-&Sia-} to identify ESCC in this cohort of CEA (-) ESCC cases (CEA < 5 ng/ml). Observations showed that our RiskScore^{Fuc-&Sia-} demonstrated outstanding diagnostic accuracy, presenting an AUC of 0.974, a sensitivity rate of 93.06%, and a specificity rate of 91.52%. In contrast, CEA showed suboptimal results, with an AUC of 0.702, a sensitivity of 73.99%, and a specificity of 60.00% in this subgroup (Fig. 4E, Table 4). This diagnostic capability is also validated in our external validation cohort with AUC value of 0.973, sensitivity of 90.48% and a specificity of 94.44% (Fig. 4F, Table 4). Overall, these results are encouraged and emphasize that our glycosylated EVs-derived miRNAs-based signature can provide a diagnostic approach with the potential to improve ESCC screening that can serve as a complement to CEA.

Table 4 Summary of diagnostic performance of glycosylated EVs-derived miRNAs-based signature for identification of CEA (-) ESCC cases in the training and validation cohorts

Variable	Training & Internal Validation cohort (ESCC = 173, HC = 165)		External Validation cohort (ESCC = 84, HC = 72)	
	CEA	Riskscore ^{Fuc-&Sia-}	CEA	Riskscore ^{Fuc-&Sia-}
AUC	0.702 (0.647-0.758)	0.974 (0.960-0.988)	0.711 (0.627-0.795)	0.973 (0.952-0.995)
SE%	73.99	93.06	72.62	90.48
SP%	60.00	91.52	70.83	94.44
AC%	67.16	92.31	71.80	92.31
PPV%	65.98	92.00	74.39	95.00
NPV%	68.75	92.64	68.92	89.47
Youden Index%	33.99	84.58	43.45	84.92

CEA (-) CEA < 5 ng/ml, AUC area under the curve, CI confidence interval, SE sensitivity, SP specificity, AC accuracy, NPV negative predictive value, PPV positive predictive value

The glycosylated EVs-derived miRNAs-based signature has a stronger ability to distinguish individuals with ESCC in the early stage (stage I & II) than the traditional marker CEA

Early detection of cancer is pivotal for improving survival rates in patients with ESCC. In this study, upon categorizing all ESCC patients into early (stage I and II) and late (stage III and IV) groups, it was noted that both groups of ESCC patients had relatively higher CEA and Riskscore^{Fuc-&Sia-} compared to non-disease controls in training cohort and external validation cohort (Fig. 5A, D). However, there was no significant difference in both levels between early and late ESCC (Fig. 5A, D). Hence, we further explored the diagnostic capability of our Riskscore^{Fuc-&Sia-} in early-stage ESCC patients systematically. Result shown that CEA demonstrated some diagnostic efficacy in both initial and advanced stage ESCC in the training cohort (all AUC < 0.80) (Fig. 5B), which was also verified in the external validation cohort (Fig. 5E). It was intriguing to observe that our glycosylated EVs-derived miRNAs-based signature yielded a remarkable AUC of 0.982 with a sensitivity of 94.60% and a specificity of 92.50% for identifying early-stage ESCC in training cohort (Fig. 5C and Table 5). The findings were consistently validated in the external validation cohort, where the Riskscore^{Fuc-&Sia-} maintained similar effectiveness, with an AUC of 0.977 (95% CI, 0.960–0.995), with a sensitivity of 91.25% and a specificity of 94.44% for diagnosis in the patients with early-stage ESCC (Fig. 5F and Table 5). It is noteworthy that our glycosylated EVs-derived miRNAs-based signature exhibited high sensitivity, potentially reducing missed diagnoses in early-stage ESCC. The outcomes underscore the effectiveness of our glycosylated EVs-derived miRNAs-based signature in accurately detecting patients across all stages of ESCC, proving particularly powerful in pinpointing those at the earliest phases of the disease.

Discussion

Given the frequent association between changes in glycosylation patterns of cells and the advancement of cancer, as well as the substantial presence of glycans in EVs derived from cancer cells [28, 29], the exploration of glycosylation patterns in tumour EVs has considerable potential for the discovery of new and dependable biomarkers that are unique to tumour-related EVs [30]. In this research, an in-depth examination of miRNA levels in tumour-derived EVs was conducted using Fuc-EVs and Sia-EVs capture strategies. Then, we established and validated three preoperative, serum-based, glycosylated EVs-derived miRNA-based panels (the Fuc-EVs-derived DEmiRNAs panel, Sia-EVs-derived DEmiRNAs panel, and Fuc-&Sia-EVs-derived DEmiRNAs panel), demonstrating exceptional precision in diagnosing individuals with ESCC. Furthermore, our Fuc-&Sia-EVs-derived DEmiRNAs panel demonstrated strong efficacy in identifying patients with early-stage ESCC, or CEA (-) ESCC patients (CEA < 5 ng/ml) from healthy controls.

The exploration of isolation methods for EVs has been extensive in various cell culture supernatants and bodily fluid samples, driven by their potential diagnostic utility in diseases [31–35]. Traditional approaches for EVs isolation focus on size and buoyancy density, including ultracentrifugation (UC), size exclusion chromatography and filtration, to name a few [36–38]. However, these approaches depending on physical properties are currently absent from effectively distinguishing tumour-derived EVs, and the extraction process is time-consuming. Nevertheless, how to efficiently enrich tumour-derived EVs miRNAs from serum is an ongoing barrier to the potential application of EVs miRNAs in ESCC detection, particularly for early-stage diagnosis.

In recent years, multiple evidence has suggested that EVs are severely glycosylated and contain high concentrations of specific glycoconjugates [39, 40]. More

Fig. 5

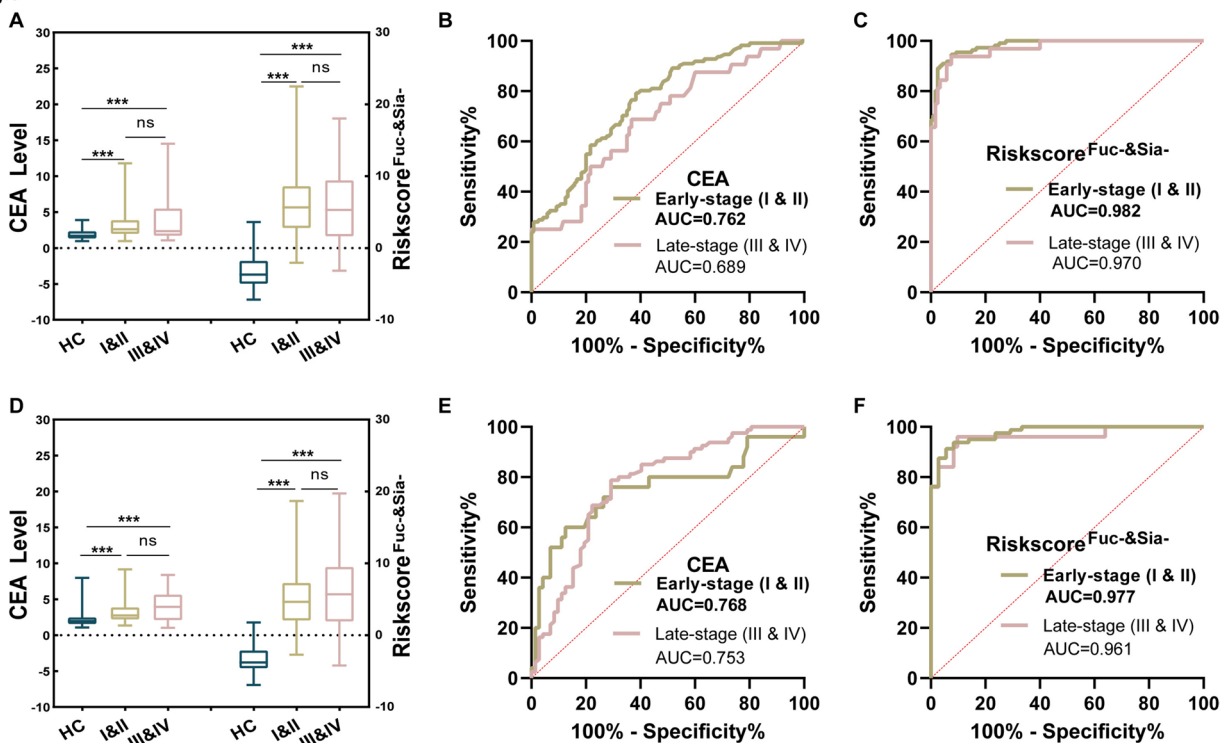


Fig. 5 The glycosylated EVs-derived miRNAs-based signature ($Riskscore^{Fuc\&Sia-}$) has a stronger ability to distinguish individuals with ESCC in the early stage (stage I & II) than the traditional marker CEA. The levels of $Riskscore^{Fuc\&Sia-}$ and CEA in healthy controls, early-stage, and late-stage patients with ESCC from the training cohort (A), and external validation cohort (D). B-C ROC curve analysis for CEA (B) or $Riskscore^{Fuc\&Sia-}$ (C) to identify early-stage (I & II), late stage (III & IV) ESCC patients from healthy controls in training cohort. E-F ROC curve analysis for CEA (E) or $Riskscore^{Fuc\&Sia-}$ (F) to identify early-stage (I & II), late stage (III & IV) ESCC patients from healthy controls in external validation cohort. ^{ns} $p > 0.05$ and ^{***} $p < 0.001$

specifically, research has demonstrated notable variations in abnormal salivation or fucosylation across various cancer types, including colon, ovarian, pancreatic, colorectal, lung, melanoma, and oral cancers [41, 42]. In addition, many studies have shown that abnormal glycosylation of EVs can affect the sorting and efflux of their cargoes [43]. It has been reported that wheat germ lectin

(WGA) has high specificity and affinity for all sialic acid bonds, including $\alpha 2, 6$ -chain, $\alpha 2, 3$ -chain, and polysialic acid [41, 42], while fucose has shown specific affinity for LCA [42]. In addition, other lectins have also shown strong ability to bind to specific glycans [44–46]. Therefore, abnormal glycosylation based on cell surface or EVs surface is a favourable biomarker. By utilizing Fuc-EVs

Table 5 Summary of early diagnostic performance of $Riskscore^{Fuc\&Sia-}$ in the training and external validation cohort

Variable	Training cohort, % (CI)		External validation cohort, % (CI)	
	CEA	$Riskscore^{Fuc\&Sia-}$	CEA	$Riskscore^{Fuc\&Sia-}$
AUC	0.762 (0.702-0.823)	0.982 (0.970-0.994)	0.768 (0.692-0.845)	0.977 (0.960-0.995)
SE%	79.28	94.60	78.75	91.25
SP%	61.67	92.50	70.83	94.44
AC%	70.13	93.51	75.00	92.76
PPV%	65.67	92.11	75.00	94.81
NPV%	76.29	94.87	75.00	90.67
Youden Index%	40.95	87.10	49.58	85.69

AUC area under the curve, CI confidence interval, SE sensitivity, SP specificity, AC accuracy, NPV negative predictive value, PPV positive predictive value

and Sia-EVs capture strategies involving specific lectins such as WGA and LCA coupled to magnetic beads, we successfully enriched tumour-derived EVs from ESCC cells, as evidenced by the notably higher particle number ratios isolated from ESCC cells as compared to those from normal cells (Additional file 1: Fig S1). Interestingly, in serum total EVs isolated by the UC method, there was no statistical difference in the expression of Fuc-&Sia-EVs-derived DEmiRNAs between normal subjects and ESCC patients (Additional file 1: FigS7), further confirming the specificity of our glycosylated EVs strategies. Furthermore, this study utilized automated extraction methods for glycosylated EVs and EVs-derived miRNAs, demonstrating efficiency, rapidity, and controllability at the experimental scale. Moreover, the adoption of RT-qPCR for miRNA analysis, recognized as the gold standard for nucleic acid quantification and commonly employed for multigene detection, enhances the translatability of our glycosylated EVs-derived miRNAs-based signature to molecular diagnostic analysis for clinical applications. Additionally, in this investigation, tumour-derived EVs were effectively isolated from serum through the LCA or WGA coated magnetic beads, which was also reflected in the enrichment of pathways in our model miRNA target genes, almost all of which are involved in the development of tumours (Additional file 1: FigS8-9). Prior research has demonstrated that EVs exhibit selective cargo enrichment, leading to distinct proteomic, transcriptomic, and lipidomic expression profiles [28]. Furthermore, the biomolecular composition of EVs varies according to their cellular origin, with notable differences observed between EVs derived from healthy and diseased states [47]. Consequently, the expression of glycosylated EVs in miRNA profiles is expected to differ significantly across various tumour types, a phenomenon corroborated by our previous investigations [26]. Consequently, this research will offer robust theoretical and empirical support for the development of early diagnostic models for multiple cancers. In addition, the development of specific drug resistance targets and the dynamic monitoring of cancer patients also have important application prospects. Collectively, our findings indicate that the technique of capture with fucose stands out for its dependability, efficiency, and ease, serving as an effective strategy for the segregation of tumour-derived EVs from serum. This finding paves the way for a potentially innovative method for the early detection of cancer (not just ESCC) through the analysis of serum glycosylated EVs miRNAs.

The isolation of glycosylated EVs, as an emerging liquid biopsy technique, presents significant challenges in clinical translation. In this study, we adopted the principles of automated nucleic acid extraction used in laboratory

settings and integrated processes such as incubation, washing, and elution. This led to the development of a high-throughput and programmable method for the separation of glycosylated EVs. This method enhances the consistency and efficiency of sample processing, thereby ensuring reliable and uniform test results across various medical institutions and establishes a robust foundation for its widespread implementation and application [26]. Currently, the primary challenge is the cost, primarily attributed to the use of high-quality lectins, which leads to a higher cost per sample compared to conventional tumour markers such as CEA and SCC-Ag in large-scale applications [7]. Nonetheless, it is anticipated that advancements in technology will address this issue. Despite these challenges, the following studies based on this technology remains feasible: 1. Development of biological targets in diverse populations: Implement recruitment strategies that encompass a wide range of patient demographics, including various age groups, genders, and geographic regions. Conduct multi-center prospective clinical studies to identify potential biomarkers or feature combinations through big data analytics, aiming to optimize diagnostic models and mitigate population bias. 2. Consideration of the overall cancer staging involves in a comprehensive focus on the entire disease trajectory. This includes the early detection of glycosylated EV micro-tumour signals to facilitate precise screening and the routine screening of high-risk populations. In the intermediate stages, it is crucial to monitor the effects of combined treatments, assess therapeutic efficacy, and predict potential recurrence. In the later stages, identifying drug resistance information is essential to support personalized treatment strategies. This approach spans all phases of diagnosis and treatment, thereby enhancing clinical value. In this study, we successfully developed a glycosylated EVs-based miRNAs model through a multi-step screening and validation process. However, we acknowledge the potential for selection bias, as certain miRNAs with relatively poor performance, such as miR-2110 and miR-582-3p, were excluded from the diagnostic model. The suboptimal performance and subsequent exclusion of these miRNAs may be attributed to biological factors, such as the disruption of expression stability within the intricate regulatory network of the tumour microenvironment, which may be influenced by tumour heterogeneity. From a technical analysis standpoint, the sample processing procedures, including systematic errors in reverse transcription and quantitative PCR amplification, may exacerbate detection noise. This noise can obscure potentially weak yet genuine miRNA signals, ultimately resulting in suboptimal diagnostic performance across different cohorts. In short, we should face up to their existence and

shortcomings, not only to provide improved targets for subsequent studies to optimize diagnostic models, but also to avoid the risk of one-sided interpretation caused by focusing only on advantageous markers.

Numerous studies have increasingly demonstrated that alterations in glycosylation are not only associated with tumour development but also contribute to tumorigenesis [41, 48–51]. For example, recent findings indicate that modifications in cell surface sialylation play a role in enhancing the metastatic and invasive potential of hepatocellular carcinoma (HCC), gastric cancer (GC), and colorectal cancer (CRC) by facilitating epithelial-mesenchymal transition (EMT) [52, 53]. Alterations in mucin sialylation have been reported to be responsible for the decline of mucosal protection, thereby contributing to the onset of gastric cancer [54]. In the context of GC, sialylation further facilitates the adhesion of *Helicobacter pylori* to the gastric mucosa, thereby promoting the progression of the disease [55]. Furthermore, elevated levels of sialylation in tumour cells can modify the expression of sialic acid-binding immunoglobulin-type lectin ligands on the surfaces of various immune cells, thereby facilitating immunosuppressive signalling and enabling cancer cells to evade detection and elimination by the immune system [41, 56, 57]. In addition to sialylation, increased fucosylation is also a prevalent characteristic observed in cancer development and progression. Recent studies have identified FUT8, an enzyme responsible for core fucosylation, as a significant driver of melanoma metastasis [58]. Furthermore, aberrant elevations of fucosylation levels in breast, colorectal, and pancreatic cancers have been shown to influence metastatic potential by enhancing tumour cell interactions with selectin-expressing leukocytes, platelets, and endothelial cells [52, 59, 60]. Although the underlying mechanisms linked to alterations in glycosylation, particularly sialylation and fucosylation, with the progression of variety of cancers are well-documented, the functional pathways and potential mechanisms regulated by abnormal glycosylation in ESCC have not yet been reported up to now, and further exploration is needed in our future study.

There are also some defects or challenges in the current study. First, although the prediction model based on glycosylated EVs-derived miRNAs has been effective in identifying cases of ESCC, the model specificity of ESCC compared to other cancer types still needs further investigation. An additional constraint of our investigation was the focus on miRNA markers found to be highly expressed only in ESCC, which may not fully represent the complexity of the disease. In addition, although the enrolled ESCC patient cohort is close to the regional epidemiological data in terms of age, gender, etc., there are

still potential bias effects. Therefore, while our miRNA panel diagnostics are effective in detecting ESCC, it is important to recognize the occurrence of false-positive outcomes in a portion of the patient population.

Conclusions

In our pioneering study, we effectively isolated and enriched tumour-specific EVs from patient serum samples using an advanced glycosylated EVs capture strategy. Building upon this initial finding, we curated a panel of seven miRNAs, shows the optimal potential as a biomarker for early detection of ESCC.

Abbreviations

Fuc-	Fucosylated
Sia-	Sialylated
LCA	Lentil lectin agglutinin
WGA	Wheat germ agglutinin
EVs	Extracellular vehicles
Glycosylated EVs	Glycosylated extracellular vehicles
miRNA	MicroRNA
DEmiRNAs	Differentially expressed miRNAs
pDEmiRNAs	Potential differentially expressed miRNAs
SCC-Ag	Squamous cell carcinoma antigen
TEM	Transmission electron microscopy
NTA	Nanoparticle tracking analysis
AUC	Area under the curve
CEA	Carcinoembryonic antigen
CI	Confidence interval
ESCC	Esophageal squamous cell carcinoma
NPV	Negative predictive value
PPV	Positive predictive value
RT-qPCR	Real-time quantitative reverse transcription polymerase chain reaction
ROC	Receiver operating characteristic curve
AJCC	American Joint Committee on Cancer

Supplementary Information

The online version contains supplementary material available at <https://doi.org/10.1186/s12916-025-03871-z>.

Supplementary Material 1: Additional File 1. The Additional File 1 include five parts, specifically: 1. The method of the main text. 2. The interpretation of the FigS1,7-9. 3. Table S4-13. 4. FigS1-9. 5. Figure Legend for FigS1-9. FigS1- [Extracellular vehicles (EVs) detection and characterization]. FigS2- [The detailed marker screening criteria and procession]. FigS3- [Candidate biomarkers were preliminary confirmed in screening cohort]. FigS4- [Differentially expressed pDEmiRNAs, CEA, SCC-Ag evaluation through the training cohort and the diagnostic capability of DEmiRNAs was evaluated]. FigS5- [Diagnostic validation and diagnostic parameter application in an independent internal validation cohort]. FigS6- [Differentially expressed DEmiRNAs, and CEA evaluation through the external validation cohort from medical centre]. FigS7- [Expression analysis of DEmiRNAs in EVs isolated by different methods]. FigS8- [Identification and enrichment exploration of the model miRNAs]. FigS9- [Functional validation of DEmiRNAs in ESCC cell lines].

Supplementary Material 1: Additional File 2. The Additional File 2 include Table S1-3 and Table S 14-16.

Acknowledgements

We would like to thank the nurses, pathologists, and patients who participated in these studies.

Authors' contributions

HJT, CDY, and YH contributed to the conception and design; JLC, YZ and ZW contributed to the provision of study materials or patients. JLC and YZ contributed to gene detection, data analysis and interpretation. XFC, NTK, JMW, XL, YHZ, ZXH, MF LLZ, HM contributed to the Resources, Data curation. FL, QG, KH contributed to draft the manuscript. All authors reviewed the manuscript.

Funding

This study was supported in part by Medical Vertical Project of Fujian Province (Grant No. 2020CXB001) to Yi Huang, Joint Fund of Science and Technology Innovation of Fujian Province (Grant No. 2021Y9024) to Yi Huang, Key Project of Natural Science Foundation of Fujian Province (Grant No. 2022J02048) to Yi Huang.

Data availability

The dataset(s) supporting the conclusions of this article is(are) included within the article and its additional file (Additional file 2: Table S1-2).

Declarations

Ethics approval and consent to participate

This study was sought and approved by the Ethics Committee of Fujian Provincial Hospital (Ethics Approval Number K2022-05-010). Informed consent was obtained from all subjects and/or their legal guardian(s). All methods were carried out in accordance with relevant guidelines and regulations.

Consent for publication

Not applicable. The manuscript does not contain any individual personal data.

Competing interests

The authors declare no competing interests.

Author details

¹Shengli Clinical Medical College, Fujian Medical University, Fujian, Fuzhou 350001, China. ²Present Address: Department of Clinical Laboratory, Fujian Provincial Hospital, Fuzhou 350001, China. ³Department of Clinical Laboratory, Shishi Hospital, Fujian 362700, Shishi, China. ⁴Research and development center, Beijing Youneng Technology Co. Ltd, Beijing 102600, People's Republic of China. ⁵Research and development center, Beijing Hotgen Biotech Co., Ltd, Beijing 102600, People's Republic of China. ⁶Department of Scientific Research, Fujian Provincial Hospital, Fujian, Fuzhou 350001, China. ⁷Department of Clinical Laboratory, the Second Affiliated Hospital, Zhejiang University School of Medicine, Zhejiang, Hangzhou 310009, China. ⁸Integrated Chinese and Western Medicine College, Fujian University of Traditional Chinese Medicine, Fujian, Fuzhou 350108, China. ⁹Department of Clinical Laboratory, Jinhua Municipal Central Hospital, Zhejiang 321000, Jinhua, China. ¹⁰Department of Thoracic Surgery, Fujian Provincial Hospital, Fujian, Fuzhou 350001, China. ¹¹Department of Geriatric Medicine, Fujian Provincial Hospital, Fujian, Fuzhou 350001, China. ¹²Fujian Provincial Centre for Geriatrics, Fujian Provincial Hospital, Fujian, Fuzhou 350001, China. ¹³Departments of Clinical Laboratory, Changzhi People's Hospital, Shanxi, Changzhi 046000, China. ¹⁴Center for Experimental Research in Clinical Medicine, Fujian Provincial Hospital, Fujian, Fuzhou 350001, China. ¹⁵State Key Laboratory of Cellular Stress Biology, Innovation Centre for Cell Signalling Network, School of Life Sciences, Xiamen University, Fujian, Xiamen 361102, China. ¹⁶Central Laboratory, Fujian Provincial Hospital, Fujian, Fuzhou 350001, China. ¹⁷Fujian Provincial Key Laboratory of Cardiovascular Disease, Fujian Provincial Key Laboratory of Critical Care Medicine, Fujian, Fuzhou 350001, China.

Received: 13 July 2024 Accepted: 14 January 2025

Published online: 23 January 2025

References

- Arnold M, Soerjomataram I, Ferlay J, Forman D. Global incidence of oesophageal cancer by histological subtype in 2012. *Gut*. 2015;64(3):381–7.
- Organization WH. Global health estimates: leading causes of death. September 26, 2021. Accessed April30,2022 2021 [Available from: [https://](https://www.who.int/data/gho/data/themes/mortality-and-global-health-estimates/ghe-leading-causes-of-death)

- www.who.int/data/gho/data/themes/mortality-and-global-health-estimates/ghe-leading-causes-of-death.
- Huang FL, Yu SJ. Esophageal cancer: Risk factors, genetic association, and treatment. *Asian J Surg*. 2018;41(3):210–5.
- Siegel RL, Miller KD, Fuchs HE, Jemal A. Cancer Statistics, 2021. *CA Cancer J clin*. 2021;71(1):7–33.
- Gao QY, Fang JY. Early esophageal cancer screening in China. *Best Pract Res Clin Gastroenterol*. 2015;29(6):885–93.
- Schmid E, Blaich E, Schwarzkopf H, Kovarik P. [Diagnostic accuracy of fiber endoscopy in esophageal and gastric carcinoma. Attempt at error analysis]. *Zeitschrift fur Gastroenterologie*. 1978;16(4):229–34.
- Mroczko B, Kozłowski M, Groblewska M, Łukaszewicz M, Nikliński J, Jelski W, et al. The diagnostic value of the measurement of matrix metalloproteinase 9 (MMP-9), squamous cell cancer antigen (SCC) and carcinoembryonic antigen (CEA) in the sera of esophageal cancer patients. *Clinica chimica acta; international journal of clinical chemistry*. 2008;389(1–2):61–6.
- Zheng Q, Zhang L, Tu M, Yin X, Cai L, Zhang S, et al. Development of a panel of autoantibody against NSG1 with CEA, CYFRA21- 1, and SCC-Ag for the diagnosis of esophageal squamous cell carcinoma. *Clin Chim Acta*. 2021;520:126–32.
- Ke W, Zeng L, Hu Y, Chen S, Tian M, Hu Q. Detection of early-stage extrahepatic cholangiocarcinoma in patients with biliary strictures by soluble B7–H4 in the bile. *Am J Cancer Res*. 2018;8(4):699–707.
- Wang X-B, Jiang X-R, Yu X-Y, Wang L, He S, Feng F-Y, et al. Macrophage inhibitory factor 1 acts as a potential biomarker in patients with esophageal squamous cell carcinoma and is a target for antibody-based therapy. *Cancer Sci*. 2014;105(2):176–85.
- Mellby LD, Nyberg AP, Johansen JS, Wingren C, Nordestgaard BG, Bojesen SE, et al. Serum Biomarker Signature-Based Liquid Biopsy for Diagnosis of Early-Stage Pancreatic Cancer. *J Clin Oncol*. 2018;36(28):2887–94.
- He J, Tan W, Ma J. Circulating tumor cells and DNA for real-time EGFR detection and monitoring of non-small-cell lung cancer. *Future oncology (London, England)*. 2017;13(9):787–97.
- Chaffer CL, Weinberg RA. A perspective on cancer cell metastasis. *Science (New York, NY)*. 2011;331(6024):1559–64.
- Sedlackova T, Repiska G, Celec P, Szemes T, Minarik G. Fragmentation of DNA affects the accuracy of the DNA quantitation by the commonly used methods. *Biological procedures online*. 2013;15(1):5.
- Ignatiadis M, Lee M, Jeffrey SS. Circulating Tumor Cells and Circulating Tumor DNA: Challenges and Opportunities on the Path to Clinical Utility. *Clinical cancer research : an official journal of the American Association for Cancer Research*. 2015;21(21):4786–800.
- Boukouris S, Mathivanan S. Exosomes in bodily fluids are a highly stable resource of disease biomarkers. *Proteomics Clin Appl*. 2015;9(3–4):358–67.
- Fan TWM, Zhang X, Wang C, Yang Y, Kang WY, Arnold S, et al. Exosomal lipids for classifying early and late stage non-small cell lung cancer. *Anal Chim Acta*. 2018;1037:256–64.
- Tauro BJ, Greening DW, Mathias RA, Ji H, Mathivanan S, Scott AM, et al. Comparison of ultracentrifugation, density gradient separation, and immunoaffinity capture methods for isolating human colon cancer cell line LIM1863-derived exosomes. *Methods (San Diego, Calif)*. 2012;56(2):293–304.
- Witwer KW, Buzás EI, Bemis LT, Bora A, Lässer C, Lötvall J, et al. Standardization of sample collection, isolation and analysis methods in extracellular vesicle research. *Journal of extracellular vesicles*. 2013;2. <https://doi.org/10.3402/jev.v2i0.20360>.
- Lange T, Samatov TR, Tonevitsky AG, Schumacher U. Importance of altered glycoprotein-bound N- and O-glycans for epithelial-to-mesenchymal transition and adhesion of cancer cells. *Carbohydr Res*. 2014;389:39–45.
- Thomas D, Rathinavel AK, Radhakrishnan P. Altered glycosylation in cancer: A promising target for biomarkers and therapeutics. *Biochim Biophys Acta Rev Cancer*. 2021;1875(1):188464.
- Lumibao JC, Tremblay JR, Hsu J, Engle DD. Altered glycosylation in pancreatic cancer and beyond. *J Exp Med*. 2022;219(6). <https://doi.org/10.1084/jem.20211505>.
- Wang L, Chen X, Wang L, Wang S, Li W, Liu Y, et al. Knockdown of ST6Gal-1 expression in human hepatocellular carcinoma cells inhibits their

- exosome-mediated proliferation- and migration-promoting effects. *IUBMB Life*. 2021;73(11):1378–91.
24. Jia L, Zhang J, Ma T, Guo Y, Yu Y, Cui J. The Function of Fucosylation in Progression of Lung Cancer. *Front Oncol*. 2018;8:565.
 25. Zhuang W, Liu C, Hong Y, Zheng Y, Huang M, Tang H, et al. Tumor-suppressive miR-4732-3p is sorted into fucosylated exosome by hnRNPk to avoid the inhibition of lung cancer progression. *Journal of experimental & clinical cancer research : CR*. 2024;43(1):123.
 26. Chen X, Yu L, Hao K, Yin X, Tu M, Cai L, et al. Fucosylated exosomal miRNAs as promising biomarkers for the diagnosis of early lung adenocarcinoma. *Front Oncol*. 2022;12:935184.
 27. Miyoshi J, Zhu Z, Luo A, Toden S, Zhou X, Izumi D, et al. A microRNA-based liquid biopsy signature for the early detection of esophageal squamous cell carcinoma: a retrospective, prospective and multicenter study. *Mol Cancer*. 2022;21(1):44.
 28. Williams C, Royo F, Aizpurua-Olaizola O, Pazos R, Boons GJ, Reichardt NC, et al. Glycosylation of extracellular vesicles: current knowledge, tools and clinical perspectives. *Journal of extracellular vesicles*. 2018;7(1):1442985.
 29. Costa J. Glycoconjugates from extracellular vesicles: Structures, functions and emerging potential as cancer biomarkers. *Biochimica et Biophysica Acta (BBA) - Reviews on Cancer*. 2017;1868(1):157–66.
 30. Vrablova V, Kosutova N, Blsakova A, Bertokova A, Kasak P, Bertok T, et al. Glycosylation in extracellular vesicles: Isolation, characterization, composition, analysis and clinical applications. *Biotechnol Adv*. 2023;67:108196.
 31. Nakamura K, Zhu Z, Roy S, Jun E, Han H, Munoz RM, et al. An Exosome-based Transcriptomic Signature for Noninvasive, Early Detection of Patients With Pancreatic Ductal Adenocarcinoma: A Multicenter Cohort Study. *Gastroenterology*. 2022;163(5):1252–66.e2.
 32. Zhong Y, Ding X, Bian Y, Wang J, Zhou W, Wang X, et al. Discovery and validation of extracellular vesicle-associated miRNAs as noninvasive detection biomarkers for early-stage non-small-cell lung cancer. *Mol Oncol*. 2021;15(9):2439–52.
 33. Seo JW, Lee YH, Tae DH, Kim YG, Moon JY, Jung SW, et al. Development and validation of urinary exosomal microRNA biomarkers for the diagnosis of acute rejection in kidney transplant recipients. *Front Immunol*. 2023;14:1190576.
 34. Yang P, Song F, Yang X, Yan X, Huang X, Qiu Z, et al. Exosomal MicroRNA signature acts as an efficient biomarker for non-invasive diagnosis of gallbladder carcinoma. *iScience*. 2022;25(9):104816.
 35. Li K, Lin Y, Zhou Y, Xiong X, Wang L, Li J, et al. Salivary Extracellular MicroRNAs for Early Detection and Prognostication of Esophageal Cancer: A Clinical Study. *Gastroenterology*. 2023;165(4):932–45.e9.
 36. Li W-J, Chen H, Tong M-L, Niu J-J, Zhu X-Z, Lin L-R. Comparison of the yield and purity of plasma exosomes extracted by ultracentrifugation, precipitation, and membrane-based approaches. *Open Chem*. 2022;20(1):182–91.
 37. Yang D, Zhang W, Zhang H, Zhang F, Chen L, Ma L, et al. Progress, opportunity, and perspective on exosome isolation - efforts for efficient exosome-based theranostics. *Theranostics*. 2020;10(8):3684–707.
 38. Zhang Y, Bi J, Huang J, Tang Y, Du S, Li P. Exosome: A Review of Its Classification, Isolation Techniques, Storage, Diagnostic and Targeted Therapy Applications. *Int J Nanomedicine*. 2020;15:6917–34.
 39. Krishnamoorthy L, Bess JW, Preston AB, Nagashima K, Mahal LK. HIV-1 and microvesicles from T cells share a common glycome, arguing for a common origin. *Nat Chem Biol*. 2009;5(4):244–50.
 40. Batista BS, Eng WS, Pilobello KT, Hendricks-Muñoz KD, Mahal LK. Identification of a Conserved Glycan Signature for Microvesicles. *J Proteome Res*. 2011;10(10):4624–33.
 41. Pinho SS, Reis CA. Glycosylation in cancer: mechanisms and clinical implications. *Nat Rev Cancer*. 2015;15(9):540–55.
 42. Miyoshi E, Moriwaki K, Nakagawa T. Biological function of fucosylation in cancer biology. *J Biochem*. 2008;143(6):725–9.
 43. Costa J. Glycoconjugates from extracellular vesicles: Structures, functions and emerging potential as cancer biomarkers. *Biochim Biophys Acta*. 2017;1868(1):157–66.
 44. Belický Š, Katrlík J, Tkáč J. Glycan and lectin biosensors. *Essays Biochem*. 2016;60(1):37–47.
 45. Gerlach JQ, Maguire CM, Krüger A, Joshi L, Prina-Mello A, Griffin MD. Urinary nanovesicles captured by lectins or antibodies demonstrate variations in size and surface glycosylation profile. *Nanomedicine (Lond)*. 2017;12(11):1217–29.
 46. Choi Y, Park U, Koo HJ, Park JS, Lee DH, Kim K, et al. Exosome-mediated diagnosis of pancreatic cancer using lectin-conjugated nanoparticles bound to selective glycans. *Biosens Bioelectron*. 2021;177:112980.
 47. Yáñez-Mó M, Siljander PR, Andreu Z, Zavec AB, Borràs FE, Buzas EI, et al. Biological properties of extracellular vesicles and their physiological functions. *Journal of extracellular vesicles*. 2015;4:27066.
 48. Caval T, Alisson-Silva F, Schwarz F. Roles of glycosylation at the cancer cell surface: opportunities for large scale glycoproteomics. *Theranostics*. 2023;13(8):2605–15.
 49. Häuselmann I, Borsig L. Altered tumor-cell glycosylation promotes metastasis. *Front Oncol*. 2014;4:28.
 50. Keeley TS, Yang S, Lau E. The Diverse Contributions of Fucose Linkages in Cancer. *Cancers*. 2019;11(9).
 51. Dobie C, Skropeta D. Insights into the role of sialylation in cancer progression and metastasis. *Br J Cancer*. 2021;124(1):76–90. <https://doi.org/10.1007/s12253-015-0033-6>.
 52. Läubli H, Borsig L. Selectins promote tumor metastasis. *Semin Cancer Biol*. 2010;20(3):169–77.
 53. Kannagi R, Izawa M, Koike T, Miyazaki K, Kimura N. Carbohydrate-mediated cell adhesion in cancer metastasis and angiogenesis. *Cancer Sci*. 2004;95(5):377–84.
 54. Corfield AP. Mucins: a biologically relevant glycan barrier in mucosal protection. *Biochem Biophys Acta*. 2015;1850(1):236–52.
 55. Zhang SZ, Lobo A, Li PF, Zhang YF. Sialylated glycoproteins and sialyltransferases in digestive cancers: Mechanisms, diagnostic biomarkers, and therapeutic targets. *Crit Rev Oncol Hematol*. 2024;197:104330.
 56. Stanczak MA, Rodrigues Mantuano N, Kirchhammer N, Sanin DE, Jacob F, Coelho R, et al. Targeting cancer glycosylation repolarizes tumor-associated macrophages allowing effective immune checkpoint blockade. *Sci Transl Med*. 2022;14(669):eabj1270.
 57. Stanczak MA, Siddiqui SS, Trefny MP, Thommen DS, Boligan KF, von Gunten S, et al. Self-associated molecular patterns mediate cancer immune evasion by engaging Siglecs on T cells. *J Clin Investig*. 2018;128(11):4912–23.
 58. Agrawal P, Fontanals-Cirera B, Sokolova E, Jacob S, Vaiana CA, Argibay D, et al. A Systems Biology Approach Identifies FUT8 as a Driver of Melanoma Metastasis. *Cancer Cell*. 2017;31(6):804–19.e7.
 59. McEver RP. Selectins: initiators of leucocyte adhesion and signalling at the vascular wall. *Cardiovasc Res*. 2015;107(3):331–9.
 60. Brown JR, Fuster MM, Li R, Varki N, Glass CA, Esko JD. A disaccharide-based inhibitor of glycosylation attenuates metastatic tumor cell dissemination. *Clinical cancer research : an official journal of the American Association for Cancer Research*. 2006;12(9):2894–901.

Publisher's Note

Springer Nature remains neutral with regard to jurisdictional claims in published maps and institutional affiliations.